ISSN: 2167-9479 Volume 12, Number 2, June 2023

Scientific Research Publishing

International Journal of Modern Nonlinear Theory and Application

ISSN: 2167-9479

https://www.scirp.org/journal/ijmnta

Journal Editorial Board

ISSN: 2167-9479 (Print) ISSN: 2167-9487 (Online)

https://www.scirp.org/journal/ijmnta

Editor-in-Chief

Editorial Board

Scientific Research Publishing

International Journal of Modern Nonlinear Theory and Application, 2023, 12, 55-80
https://www.scirp.org/journal/ijmnta
ISSN Online: 2167-9487
ISSN Print: 2167-9479

Table of Contents

Volume 12 Number 2 June 2023

International Journal of Modern Nonlinear Theory and Application (IJMNTA)
Journal Information

SUBSCRIPTIONS

The *International Journal of Modern Nonlinear Theory and Application* (Online at Scientific Research Publishing, https://www.scirp.org/) is published quarterly by Scientific Research Publishing, Inc., USA.

Subscription rates:
Print: $59 per issue.
To subscribe, please contact Journals Subscriptions Department, E-mail: sub@scirp.org

SERVICES

Advertisements
Advertisement Sales Department, E-mail: service@scirp.org

Reprints (minimum quantity 100 copies)
Reprints Co-ordinator, Scientific Research Publishing, Inc., USA.
E-mail: sub@scirp.org

COPYRIGHT

PRODUCTION INFORMATION

For manuscripts that have been accepted for publication, please contact:
E-mail: ijmnta@scirp.org

Scientific Research Publishing

International Journal of Modern Nonlinear Theory and Application, 2023, 12, 55-67
https://www.scirp.org/journal/ijmnta
ISSN Online: 2167-9487
ISSN Print: 2167-9479

Turing Instability of Gray-Scott Reaction-Diffusion Model with Time Delay Effects

Suqi Ma

Department of Mathematics, China Agricultural University, Beijing, China
Email: caumasuqi@163.com

How to cite this paper: Ma, S.Q. (2023) Turing Instability of Gray-Scott Reaction-Diffusion Model with Time Delay Effects. *International Journal of Modern Nonlinear Theory and Application*, **12**, 55-67.
https://doi.org/10.4236/ijmnta.2023.122004

Received: March 10, 2023
Accepted: June 13, 2023
Published: June 16, 2023

Abstract

The reaction diffusion Gray-Scott model with time delay is put forward with the assumption of Neumann boundary condition is satisfied. Based on the Turing bifurcation condition, the Turing curves on two parameter plane are discussed without time delay. The normal form is computed via applying Lyapunov-Schmidt reduction method in system of PDE, and the bifurcating direction of pitchfork bifurcation underlying codimension-1 singularity of Turing point is computed. The continuation of Pitchfork bifurcation is simulated with varying free parameter continuously near the turing point, which is in coincidence with the theoritical analysis results. The wave pattern formation in the case of turing instability is also simulated which discover Turing oscillation phenomena from periodicity to irregularity.

Keywords

Reaction Diffusion, Turing Bifurcation, Normal Form, Time Delay

1. Introduction

Reaction diffusion model is ubiquitous in describing the spatial-temporal dynamical evolutionary behavior and to discover a variety of wave patterns which as often are seen in biological species in real life. The Gray-Scott diffusion model is motivated to do such simulations and have attracted attention in many researchers investigation work. Initially it was set forth by Gray and Scott as a variant of the autocatalytic model of glycolysis proposed by Sel'kov. Later authors in the papers ([1] [2] [3] [4]) put forth its new reaction mechanism by an auto-catalytic sequence and modelling its state variable control by time delay feedback method. For simplicity, the Gray and Scott model comes from mathemati-

cally model governed by

$$\begin{aligned}\frac{\mathrm{d}u_1}{\mathrm{d}t} &= \varepsilon d\Delta u_1 + a - u_1 - \frac{4u_1(t-\tau)u_2(t-\tau)}{1+u_1(t-\tau)^2}\\ \frac{\mathrm{d}u_2}{\mathrm{d}t} &= d\Delta u_2 + bu_1 - b\frac{u_1(t-\tau)u_2(t-\tau)}{1+u_1(t-\tau)^2}\end{aligned} \tag{1.1}$$

with the initial conditions and Neumann boundary condition

$$\begin{aligned}&\frac{\partial u_1}{\partial n} = \frac{\partial u_2}{\partial n} = 0, \quad x \in \partial\Omega, t > 0\\ &u_1(x,\theta) = \phi_1, u_2(x,\theta) = \phi_2, \quad x \in \Omega, \theta \in [-\tau, 0]\end{aligned} \tag{1.2}$$

where a, b, d, ε are constants, Δ is Laplacian operator and Ω is the domain of space variable *x*.

It is easily to calculate that Equation (1.1) has a homogeneous stationary solution

$$u_1 = \frac{ab}{b+4\sigma}, u_2 = \frac{\sigma\left(a^2b^2 + b^2 + 8b\sigma + 16\sigma^2\right)}{b(b+4\sigma)^2} \tag{1.3}$$

Motivated by the aims to discover the complex dynamical evolution behavior both of the inhomogeneous solutions, we investigate the turing bifurcation mechanism inherently with time delay effects. Lyapunov-Schmidt method can be applied to investigate the bifurcation behavior at the Turing-instability bifurcation point with simple eigenvalue. Some authors as referring to the papers ([5] [6] [7] [8]) also develop the numerical algorithm of Lyapunov-Schmidt method to explore the bifurcation scenario near simple bifurcation point. According to Lyapunov-Schmidt Reduction method, the original partial delay differential equation is expressed on the invariant center manifold to acquire the norm form correspondingly. With the analyzing results of the characteristic equation, for example the roots with zero real part crossing imaginary axis underlying the related positive or negative transversal conditions, the turing bifurcation mechanism is exploited ([9] [10] [11] [12]). The numerical simulation results verify the analyzing result and near the threshold value the simulation bifurcating solution is in coincidence with its bifurcating directions.

We get the periodical solutions in space near the turing bifurcation point and time-periodically solution mainly dependent on a series of DDEs by discretion method underlying time delay. The dynamics of Turing patterns in one dimension are simulated, which reflects the spatio-temporal oscillation under time delay feedback. The wave simulations of reaction diffusion equation with time delay still take some interesting methods, which alike the well known differential quadrature algorithms ([5] [13] [14] [15] [16]), element free Galerkin method, and Trigonometric B-spline functions interpolation method, etc. With free parameters varying in Turing instability region, the periodical travelling wave pattern is induced ([17] [18]), and even from periodicity to un-regularity of wave patterns are discovered.

The whole paper is arranged as the listed. In section 2, the turing instability of Gray and Scott model underlying time delay is discussed. In section 3, the pitchfork bifurcation branch of turing bifurcation is discussed, which also determine the bifurcation direction in turing point. In section 4, the numerical simulation is done, the results is in coincidence with the theoretical analysis proof. Finally the discussion is given briefly.

2. Turing Instability

To solve Turing bifurcation problem, we first explains some notations in diffusion Equation (1.2). Suppose X is the domain of Laplacian operator and respectively, X, Y is Hilbert space defined by the inner product $(\phi,\psi)=\int_{\Omega}\phi(\pi x)^{\mathrm{T}}\psi(\pi x)\mathrm{d}x$ wherein ϕ is defined in $\Omega=[0,1]^n$ with $n\le 3$. Mapping $G_{1,2}:(X,\alpha)\to Y$ with $\alpha\in R^2$, we write the elliptic Equation of (1.2) as

$$\begin{aligned} G_1(u,v) &= \varepsilon d\Delta u_1 + a - u_1 - \frac{4u_1u_2}{1+u_1^2} \\ G_2(u,v) &= d\Delta u_2 + bu_1 - b\frac{u_1u_2}{1+u_1^2} \end{aligned} \tag{2.1}$$

with $(u,v)\in X$ and $\alpha=(\varepsilon,d)$.

Notice we set time delay $\tau=0$ in Equation (2.1), the discussion of Turing instability of Equation (2.1) is independent of time delay. The turing-Hopf instability induce the periodical spatial oscillation phenomena doesn't discuss here, however it may happen with time delay varying due to complex wave pattern phenomena.

To analyze turing bifurcation point, we firstly investigate the characteristic equation with simple zero root. Based on the known knowledge of diffusion equation, the characteristic equation of Equation (2.1) is written as $\prod_{k=0}^{N}W_k(\lambda)=0$, with different $k\in N_0$. It is easily to compute that

$$\begin{aligned} W_k(\lambda) &= \left(\left(-4dk^2\pi^2-4\lambda\right)a^2+5b\left(d\varepsilon k^2\pi^2+\lambda+5\right)a+100dk^2\pi^2+100\lambda\right) \\ &\quad +\left(a^2+25\right)\left(dk^2\pi^2+\lambda\right)\left(d\varepsilon k^2\pi^2+\lambda+1\right) \\ &= 0 \end{aligned} \tag{2.2}$$

Turing instability expands the non-homogeneous solution bifurcation branches with spectral assumption at singularity point. The characteristic equation with zero root with $k=0$ is called as long wave modulation, however the named Turing instability happens if zero root appears with $k\ge 1$. We set

$$\begin{aligned} Tr &= \frac{a^2d\varepsilon k^2+a^2dk^2+25d\varepsilon k^2+5ab+25dk^2-3a^2+125}{a^2+25}, \\ Det &= \frac{a^2d^2\varepsilon k^4+5abd\varepsilon k^2+25d^2\varepsilon}{a^2+25} \\ &\quad +\frac{k^4-4a^2dk^2+25ab+100dk^2+dk^2a^2+25dk^2}{a^2+25}. \end{aligned} \tag{2.3}$$

As often as simple, we discuss the turing instability in the sequel paper which

satisfy with the following two assumption,

H_0: The parameters b lying in the regime above the curve $5ab-3a^2+125>0$;

H_1: The necessary condition $-15625-9a^4+130a^3b\varepsilon+\left(-25b^2\varepsilon^2+750\right)a^2+1250ab\varepsilon<0$ is satisfied since $Det_{\min}(d)<0$.

To further compute the turing point, we solve $Det=0$ to get turing curves

$$\begin{aligned} d_{k,0} &= \frac{1}{2}\frac{-5ab\varepsilon+3a^2-125+\sqrt{25a^2b^2\varepsilon^2-130a^3b\varepsilon+9a^4-1250ab\varepsilon-750a^2+15625}}{\varepsilon\left(a^2+25\right)k^2\pi^2}, \\ d_{k,1} &= \frac{1}{2}\frac{-5ab\varepsilon+3a^2-125+\sqrt{25a^2b^2\varepsilon^2-130a^3b\varepsilon+9a^4-1250ab\varepsilon-750a^2+15625}}{\varepsilon\left(a^2+25\right)k^2\pi^2} \end{aligned} \tag{2.4}$$

The turing-turing bifurcation also occurs at $\left(b^*,d^*\right)$ by setting $d_{k+1,0}=d_{k,1}$ to have

$$\begin{aligned} b_k^* = {} & \frac{5\left(2a^2k^2+2a^2k+a^2+50k^2\right)\left(2k^2+2k+1\right)}{10k^2\left(k+1\right)^2a\varepsilon}+\frac{3a^2-125}{5a\varepsilon} \\ & +\frac{2\sqrt{10}\sqrt{\left(a^2+25\right)\left(k^4+2k^3+\frac{13}{8}k^2+\frac{5}{8}k+\frac{5}{32}a^2+\frac{125}{8}\left(k+\frac{1}{2}\right)^2\right)}\left(2k^2+2k+1\right)}{5k^2\left(k+1\right)^2a\varepsilon} \end{aligned} \tag{2.5}$$

By the above discussion, $Det=0$ has a simple threshold curve $d=d(\varepsilon)$ of Turing bifurcation as depicted by Equation (2.4) if and only if $b_{*,k}<b<b_k^*$. We also compute the transversal condition

$$\frac{\mathrm{d}\lambda}{\mathrm{d}b}=\frac{-k^2\pi^2\left(a^2+25\right)(\varepsilon+1)d(\varepsilon)+3a^2-5ab-125}{k^2\pi^2\left(\left(a^2+25\right)d(\varepsilon)k^2\pi^2+5ab\right)d(\varepsilon)}<0 \tag{2.6}$$

Therefore we obtain the following results:

Proposition 2.1 With fixed parameter a,b,ε, the sequel points tracking on the Turing bifurcation curves has $d_{k,0}<d_{k,1}$ by Equation (2.4), for all positive integer k. However, turing-turing bifurcation occurs if and only if $d_{k+1,0}=d_{k,1}$ for some $k>1$, therefore, the stability property of the homogeneous solution of system (1.1) (or system (2.1)), is changed when parameters pass over the Turing bifurcation curves, and the Turing instability regions are partitioned from the stability region.

For example, choosing $a=20,b=12$, and by satisfying the basic assumptions H_0 and H_1, the turing bifurcation curves are drawn as shown in **Figure 1(a)** whilst ε lying below $\varepsilon^*=0.91365064e-1$. It is seen that the steady state is usually asymptotically stable if $\varepsilon>\varepsilon^*$. The alike conclusion is satisfied for $a=20,\varepsilon=0.05565$, and we get the turing instability region given that the parameter b below the line $b=b^*=19.70136134$. The Turing bifurcation curves are plotted as shown in **Figure 1(b)**.

3. Pitchfork Bifurcation Branch from Turing Point

As discussed in section 2, if Turing condition is satisfied, the non-constant

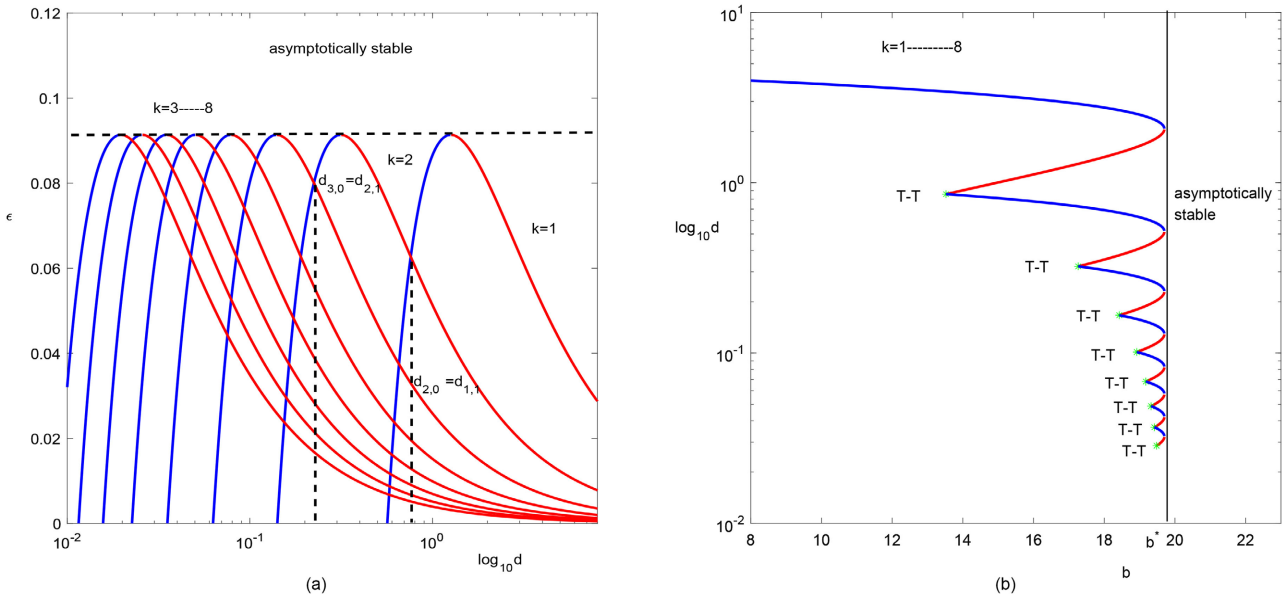

Figure 1. The turing bifurcation of parabolic Equation (2.1). (a) The Turing bifurcation curve on d-ε plane with fixed parameters as $a=20, b=12$. (b) The Turing bifurcation curve on b-d plane with fixed parameters as $a=20, \varepsilon=0.05565$. The interaction point which satisfies Equations (2.4) and (2.5) is happened with turing-turing bifurcation of codimension 2 sigularity.

steady solution arise from the Turing point. We give a description of Pitchfork solution branch bifurcating from Turing point which is also verified by germ's strong equivalent property. To clarify the bifurcating solution classifying problem, we conclude the following proposition:

Proposition 3.1 Suppose on some neighborhood $\mathcal{B}_{x,\lambda}$ of the trivial solution, we define a function $g: R^2 \to R$ which is C^∞, then a germ $g \in \mathcal{B}_{x,\lambda}$ is strongly equivalent to polynomial $\alpha x^3 \pm \beta\lambda x$ if and only if at $(x,\lambda)=(0,0)$,

$$g = \frac{\partial g}{\partial x} = \frac{\partial^2 g}{\partial x^2} = \frac{\partial g}{\partial \lambda} = 0$$

$$\alpha = sign\frac{\partial^3 g}{\partial x^3}, \quad \beta = sign\frac{\partial^2 g}{\partial \lambda \partial x}$$

Suppose $\alpha = \alpha_0$ is the bifurcation point of singularity. To discuss the stability property of the homogeneous steady state (u_*, v_*), by doing axis transformation $u = u_1 + u_*$, $v = u_2 + v_*$, $\alpha = \alpha_0 + \lambda$, the corresponding parabolic system is written as the addition of the linear system $L(u_1, v_1, \lambda)$ and the corresponding nonlinear term $N(u_1, v_1, \lambda)$, that is

$$G(u_1, v_1, \lambda) = L(u_1, v_1, \lambda) + N(u_1, v_1, \lambda) \tag{3.1}$$

with

$$L(u_1, v_1, \lambda) = \begin{pmatrix} \Delta u_1 \\ \Delta v_1 \end{pmatrix} + \begin{pmatrix} \frac{3a^2-125}{a^2+25} & \frac{-20a}{a^2+25} \\ \frac{2ba^2}{a^2+25} & \frac{-5ba}{a^2+25} \end{pmatrix} \begin{pmatrix} u_1 \\ v_1 \end{pmatrix} \tag{3.2}$$

and

$$N(u_1,v_1,\lambda) = \begin{pmatrix} -\dfrac{20a(a^2-75)}{(a^2+25)^2}u_1^2 + \dfrac{100a^2-2500}{(a^2+25)^2}u_1u_2 + \dfrac{100a^4-15000a^2+62500}{(a^2+25)^3}u_1^3 - \dfrac{500a(a^2-75)}{(a^2+25)^3}u_1^2u_2 + o(u_1+u_2)^3 \\ -\dfrac{5ba(a^2-75)}{(a^2+25)^2}u_1^2 + \dfrac{25a^2b-625b}{(a^2+25)^2}u_1u_2 + \dfrac{25b(a^4-150a^2+625)}{(a^2+25)^3}u_1^3 - \dfrac{125ba(a^2-75)}{(a^2+25)^3}u_1^2u_2 + o(u_1+u_2)^3 \end{pmatrix} \tag{3.3}$$

To compute the norm form near $(0,0)$, considering the linear operator $L(u_1,v_1,\lambda)$, the corresponding Fredholm operator should has index zero, and we have the following proposition:

Proposition 3.2 Underlying the sigularity condimension 1 bifurcation at Turing point $\alpha=\alpha_0$ in system (1.2), the normal form of Equation (2.7) undertakes its strong equivalent form which can be expressed as $g=x^3+\lambda x$. In addition, the Turing bifurcation is a supercitial Pitchfork if $\lambda<0$, or either manifies a subcritical Pitchfork if $\lambda>0$.

Hence after the recognition of normal form problem arising from Turing bifurcation with simple zero characteristic root is solved.

Proof: To carry out the normal form computation, we split space as

$$X = Ker(L)+M, \quad Y = R(L)+N \tag{3.4}$$

With $Ker(L)$ and $R(L)$ are respectively the kernal space and the range space of linear operator *L*.

For example $Ker(L)=\{\beta\phi \mid \beta\neq 0\}$, ϕ is the unit eigenvector with

$$\phi = \sqrt{2}\cos(k\pi x)\begin{pmatrix} dk^2\pi^2(a^2+25)+5ba \\ 2ba^2 \end{pmatrix}^{\mathrm{T}}$$

On the center manifold, define the projection mapping $E: Y\to N$ which can separate Equation (2.7) into

$$EG(u_1,v_1,\lambda)=0 \tag{3.5}$$

and the corresponding bifurcation equation

$$(I-E)G(u_1,v_1,\lambda)=0 \tag{3.6}$$

By the space decomposition, we write $\begin{pmatrix} u_1 \\ v_1 \end{pmatrix} = x\phi + W$, substituting it into Equation (2.9) and noticed that $EL=0$ to get $g: Ker(L)\times M\times R\to N$,

$$\begin{aligned} g(x,\lambda) &= \langle \psi, G(x\phi+W)\rangle = \langle \psi, L(x\phi+W)+N(x\phi+W)\rangle \\ &= \langle \psi, L_{\alpha 0}\phi\rangle x + \langle \psi, N(x\phi+W)\rangle \end{aligned} \tag{3.7}$$

with definition of $L_\alpha = (L_\varepsilon, L_d)^{\mathrm{T}}$ while regard the bifurcation point as

$$L_\alpha = (L_\varepsilon, L_d)^{\mathrm{T}}$$

or

$$L_\alpha = (L_\varepsilon, L_b)^{\mathrm{T}}$$

alike the definition at the turing point $L_\alpha = (L_\varepsilon, L_b)^{\mathrm{T}}$ respectively.

It is easily to compute that

$$L_b = \begin{pmatrix} 0 & 0 \\ \dfrac{2a^2}{a^2+25} & \dfrac{-5a}{a^2+25} \end{pmatrix}$$

or

$$L_d = -k_0^2\pi^2 \begin{pmatrix} \varepsilon & 0 \\ 0 & 1 \end{pmatrix}$$

We write the bifurcation equation as

$$h(x,\lambda) = (I-E)G(x\phi+W) = LW + N(x\phi+W) - \phi\langle \psi, N(x\phi+W)\rangle = 0 \quad (3.8)$$

Since the operator L is Fredholm index 0, $L: M \to R(L)$ is invertible mapping. Hence by the implicit function theorem, Equation (3.8) determines the unique expression $W = W(x,\lambda)$, then by Equation (3.7) we get the reduction equation on the center manifold

$$g(x,\lambda) = \langle \psi, N(x\phi + W(x,\lambda))\rangle \quad (3.9)$$

To verify the strong equivalent form of germ g in proposition 3.1, suppose L^* being adjoint operator of L, we can choose

$$\psi = \frac{\sqrt{2}}{\left(dk^2\pi^2\left(a^2+25\right)+5ba\right)^2 - 40ba^3}\cos(k\pi x)\begin{pmatrix} dk^2\pi^2\left(a^2+25\right)+5ba \\ -20a \end{pmatrix}^{\mathrm{T}}$$

Underlying Neumamn boundary condition, we compute $g_{xx} = 0$, and

$$\begin{aligned} g_{x\lambda} &= \langle \psi, L_\alpha \phi\rangle x\lambda, \\ g_{xxx} &= \langle psi, d^3N(0,0)(\phi,\phi,\phi)\rangle x^3, \end{aligned} \quad (3.10)$$

Therefore, the normal form in Proposition 3.2 is verified and the pitchfork bifurcation direction is determined by the sign of $\lambda = \dfrac{g_{x\lambda}}{g_{xxx}}$.

4. Numerical Simulation

Based on the results in section 2 and section 3, we can compute the corresponding Turing point via varying free parameters. For example, by simple calculation, the Turing bifurcation happens at the homogeneous equilibrium solution with chosen parameters $a = 20$, $b = 16$, $\varepsilon = 0.05565$ whilst $k = 1$, $d = 1.1181$, and from the above discussion in section 3, we can compute the base ϕ of kernal of linear operator L as $\phi = \cos(k\pi x)\begin{pmatrix} 0.44103 \\ 0.89749 \end{pmatrix}$, which further derive the formula $g(x, d_\varepsilon) = 0.4001062699e - 1x^3 + 0.8362161555d_\varepsilon x$, then the nonhomogeneous steady state solution branch bifurcates from Turing point in accordance with the direction $d_\varepsilon < 0$, which is pitchfork and subcritical bifurcation. However with $k = 2$, $d = 0.7764$, we have $g(x, d_\varepsilon) = 0.1050273688x^3 - 1.282881210d_\varepsilon x$,

which is supercritical pitchfork of Turing bifurcation. Choosing $a=20$, $\varepsilon=0.05565$ to get Turing point $k=1$, $d=1$, $b=14.96776630$ and $k=2$, $d=0.83$, $b=14.40714340$, the normal form at two different bifurcation point are respectively $g\left(x,b_\varepsilon\right)=0.3884830554e-1x^3-0.1144224171b_\varepsilon x$ and $g\left(x,b_\varepsilon\right)=0.1191247571x^3-0.4528851324e-1b_\varepsilon x$, which is Turing subcritical bifurcation. As shown in **Figure 2(a)**, with fixed parameters $a=20$, $\varepsilon=0.05565$, $b=16$, the continuation of Turing bifurcation is carrying out with the continuous varying of parameter d, which illustrates the Turing bifurcation point at $d=1.1181$ which is subcritical. As shown in **Figure 2(b)**, the parameters are fixed as $a=20$, $\varepsilon=0.05565$, $d=1$, we vary parameter b continuously, the continuation of supercritical Turing bifurcation at $b=14.96776630$ is simulated. The simulation algorithms are as often familiar as the well known differential quadrature algorithms, element free Galerkin method, and trigonometric B-spline functions interpolation method, etc.

The temporal-spatial solutions near Turing points as shown in **Figure 3** illustrate the direction of pitchfork bifurcation, which is in coincidence with the sign of the coefficients λ in normal form. For example, fixed parameter with $a=20$, $b=16$, $\varepsilon=0.05565$, as shown in **Figure 3(a)** and **Figure 3(b)**, the subcritical Turing bifurcation happens at $d=1.1181$. The constant steady state is asymptotically stable at $d=1.1190$ and the non-homogeneous solution is observed at $d=1.1080$. The supercritical Turing bifurcation manifests bifurcating non-constant solution at $d=0.7804$ as shown in **Figure 3(c)**, however the constant steady state is stable at $d=0.7704$ as shown in **Figure 3(d)**. The Turing solution and the Turing oscillation solution are observed at $\tau=0.05$, $d=0.78$ and $\tau=0.07$, $d=1.112$, as shown in **Figure 3(e)** and **Figure 3(f)**, respectively.

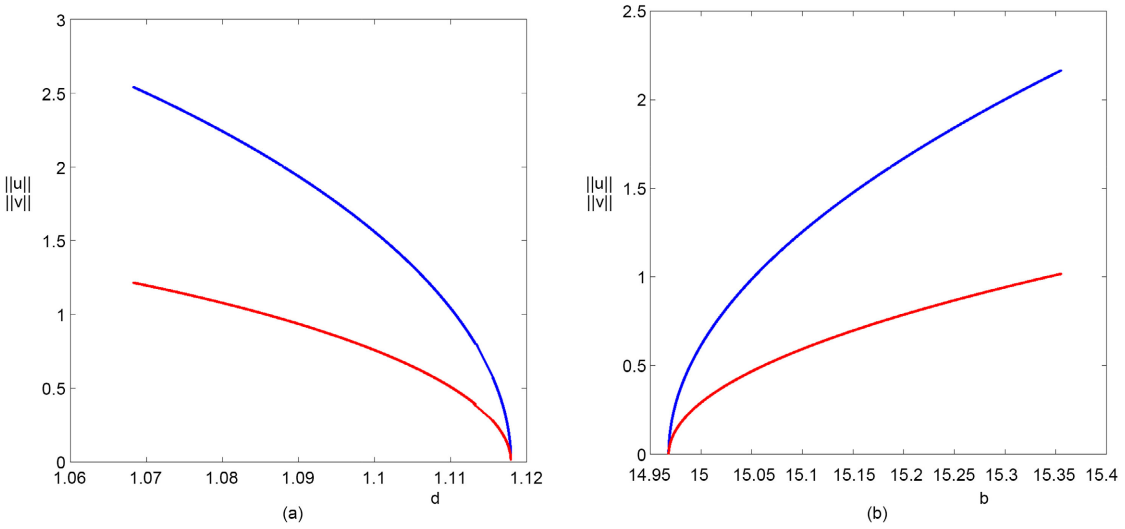

Figure 2. The continuation of turing bifurcation with $a=20$, $\varepsilon=0.05565$. (a) Chosen with $b=16$, the subcritical turing bifurcation happens at $d=1.1181$; (b) Chosen with $d=1$, the supercritical turing bifurcation happens at $b=14.96776630$.

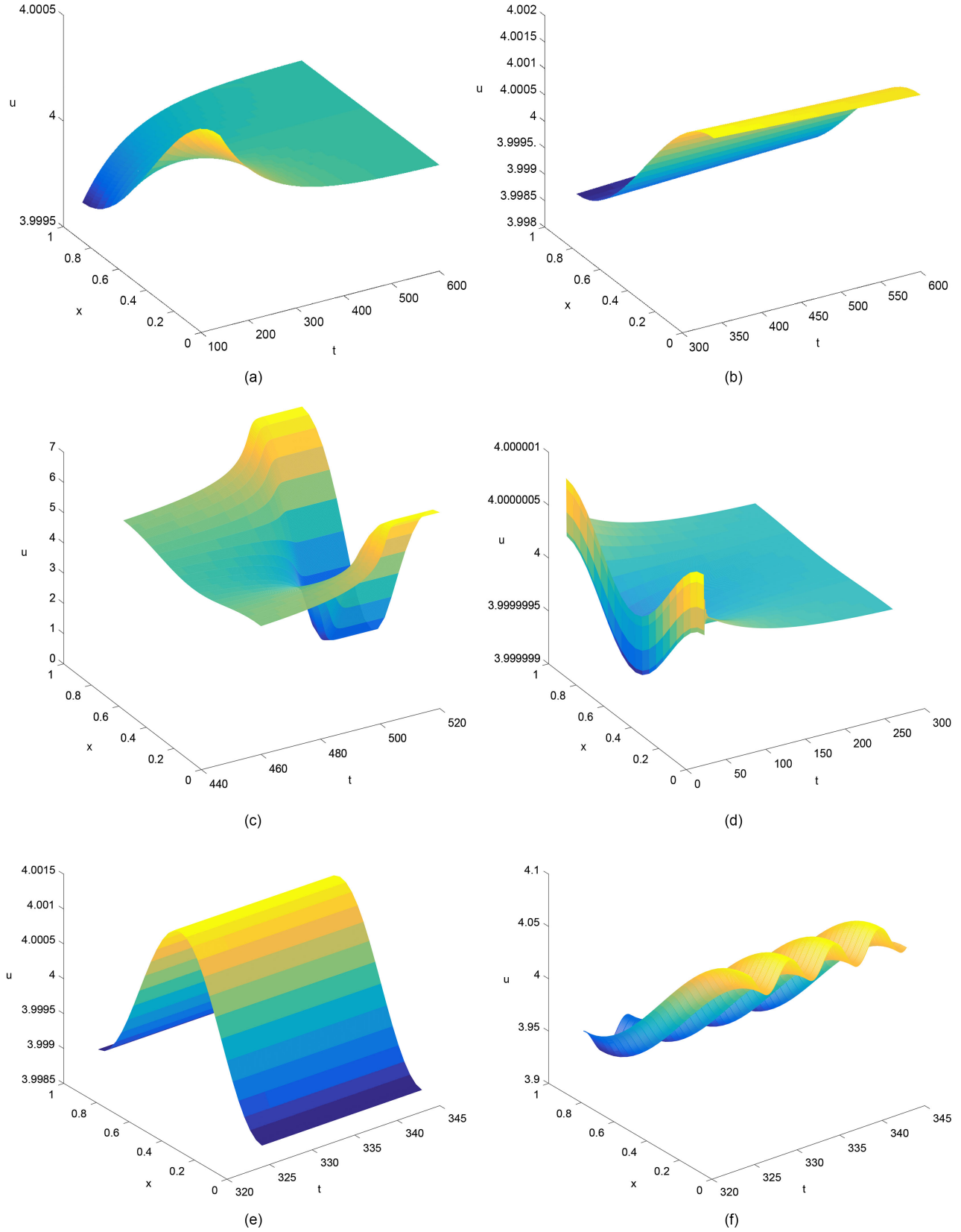

Figure 3. The supercritical turing bifurcation with $a=20$, $b=16$, $\varepsilon=0.05565$ and (a) $d=1.1190$, (b) $d=1.1080$; The subcritical turing bifurcation with (c) $d=0.7804$; (d) $d=0.7704$; (e) $\tau=0.05$, $d=0.78$ (f) $\tau=0.07$, $d=1.112$.

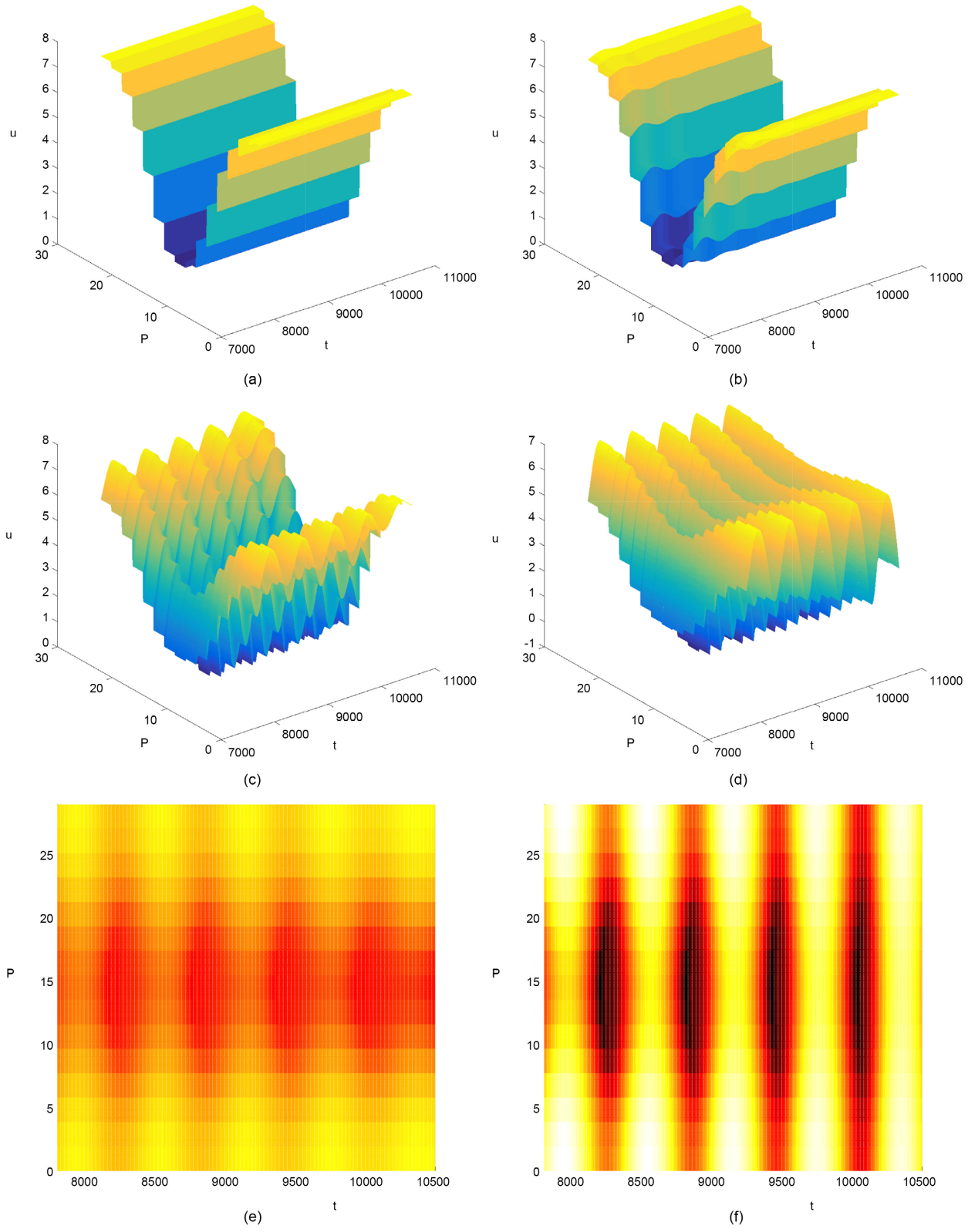

Figure 4. The turing bifurcation and turing oscillation occurs via varying time delay, the parameters are fixed with $a=20$, $b=12$, $\varepsilon=0.04565$, $d=0.89$. (a) Nonhomogeneous solution occurs with $\tau=0$; (b) The turing oscillation solution with $\tau=0.04$; (c) The turing oscillation solution with $\tau=0.049$; (d) The turing oscillation solution with $\tau=0.0498$; (e) The wave pattern with $\tau=0.049$; (f) The wave pattern with $\tau=0.0498$.

We also simulate the 2D tempo-spatial solutions and produce pictures via stretching *y*-axis in accordance with *x*-axis direction, which show us the numerical solutions of PDE in an easy way, as shown in **Figures 4(a)-(d)**. With fixed parameter $a=20$, $b=12$, $\varepsilon=0.04565$, $d=0.89$, varying time delay, system (1.1) manifests the nonhomogeneous solution at $\tau=0$, however, the occurrence of the Turing oscillation are simulated at $\tau=0.04$, $\tau=0.049$ and $\tau=0.0498$, respectively. The periodical wave patterns are schemed by projection onto X-Y plane hence is given in **Figure 4(e)** and **Figure 4(f)**.

We further do simulation to verify the wave pattern formation in Gray-Scott diffusion model with time delay effects. We choose $\tau=0.4$, fixed parameters with $a=20$, $b=9.6$, the wave pattern formation is simulated which illustrates the route of periodical oscillation to chaos, as shown in **Figures 5(a)-(d)**, With different value of ε and d, from its periodicity to irregularity, the wave patterns underlying Turing oscillation are simulated, which manifests turing-turing bifurcation can bring complex dynamical behavior underlying time delay effects.

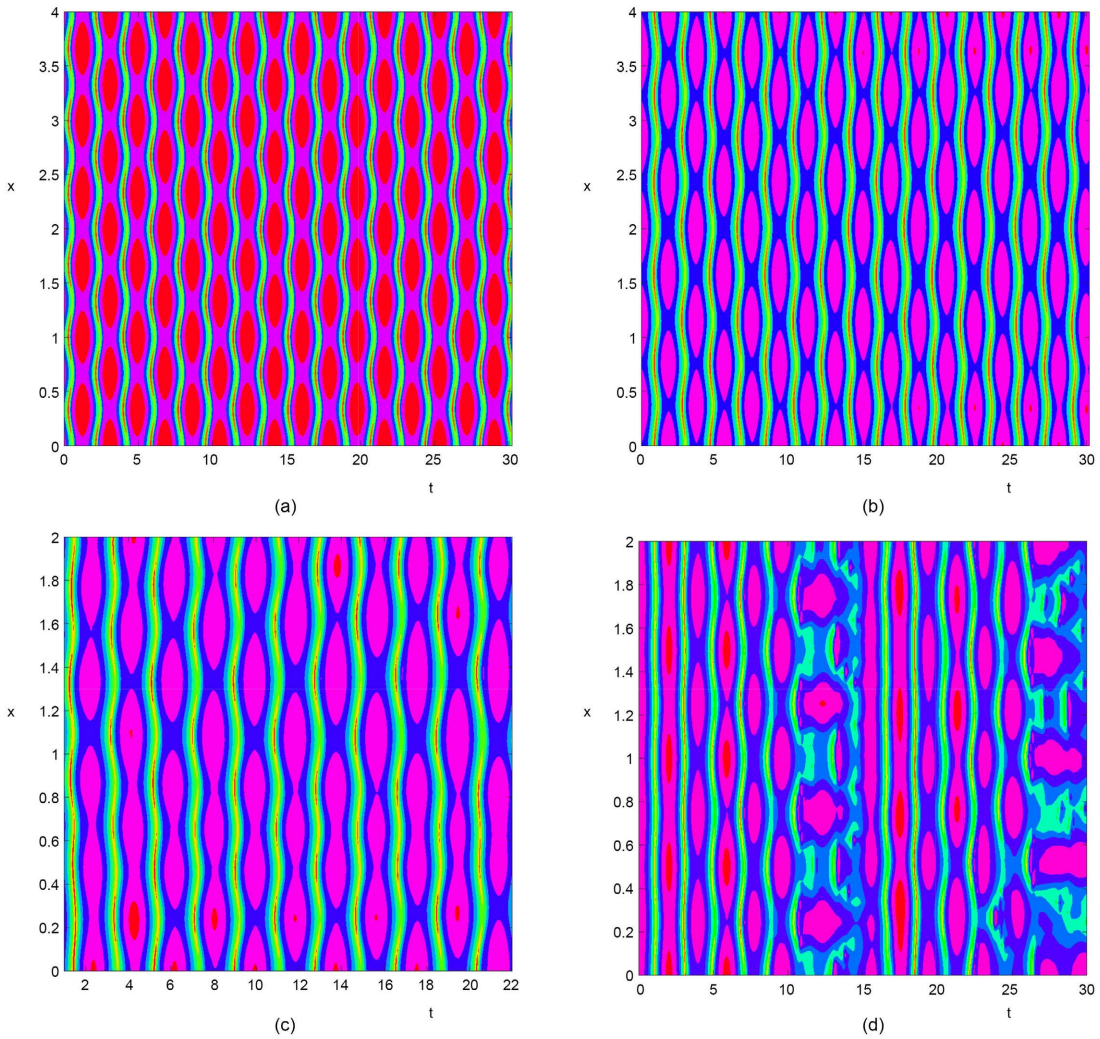

Figure 5. The wave pattern formation with $a=20$, $b=9.6$ and (a) $\varepsilon=0.02$, $d=0.4565$, (b) $\varepsilon=0.018$, $d=0.3565$; (c) $\varepsilon=0.015$, $d=0.35$; (d) $\varepsilon=0.01565$, $d=0.3$.

5. Discussion

We discuss the dynamics in Gray-Scott diffusion model produced via turing bifurcation, which usually emphasis on the significant turing condition. In an obvious way, the turing-turing bifurcation can be either independent on time delay. Underlying small time delay, the Gray-Scott diffusion model brings forth the rich formation of wave patterns. By applying Lyapunov-Schimdt reduction method, the normal form of the turing bifurcation was computed. Correspondingly, the pitchfork bifurcation direction is determined by the coefficients of the strong equivalent form of germs in R^2. However, the turing oscillation was observed as ascending time delay, which discovers that system of PDE may manifest codimesion-2 singularity and the bifurcation mechanism need to be further studied.

Acknowledgements

Sincere thanks to the members of IJMNTA for their professional performance, and special thanks to managing editor for a rare attitude of high quality.

Conflicts of Interest

The author declares no conflicts of interest regarding the publication of this paper.

References

[1] Smith, H. (2011) An Introduction to Delay Differential Equations with Applications to the Life Sciences. Springer, Berlin. https://doi.org/10.1007/978-1-4419-7646-8

[2] Kuang, K. (1992) Delay Differential Equations with Application in Population Dynamics. Springer, New York.

[3] Skalski, G. and Gilliam, J.F. (2002) Functional Responses with Predator Interference: Viable Alternatives to the Holling Type II Model. *Ecology*, **82**, 3083-3092. https://doi.org/10.1890/0012-9658(2001)082[3083:FRWPIV]2.0.CO;2

[4] Jeschke, J., Kopp, J.M. and Tollrian, R. (2002) Predator Functional Responses: Discriminating between Handling and Digesting Prey. *Ecological Monographs*, **72**, 95-112. https://doi.org/10.1890/0012-9615(2002)072[0095:PFRDBH]2.0.CO;2

[5] Chang, S.L. and Jeng, B.W. (2007) Liapunov Schmidt Reduction and Continuation for Nonlinear Schordinger Equations. *SIAM Journal on Scientific Computing*, **29**, 729-755. https://doi.org/10.1137/050642861

[6] Bohmer, K. (1993) On a Numerical Liapunov-Schmidt Method for Operator Equations. *Computing*, **51**, 237-269. https://doi.org/10.1007/BF02238535

[7] Bohmer, K. and Mei, Z. (1990) On a Numerical Liapunov-Schmidt Method. In: Allgower, E.L. and Georg, K., Eds., *Computational Solution of Nonlinear Systems of Equations*, *Lectures in Applied Mathematics*, Vol. 26, 79-98.

[8] Ashwin, P., Bohmer, K. and Mei, Z. (1995) A Numerical Liapunov-Schmidt Method with Applications to Hopf Bifurcation on a Square. *Mathematics of Computation*, **64**, 649-670. https://doi.org/10.1090/S0025-5718-1995-1284661-X

[9] Shi, H.B., Li, W.T. and Lin, G. (2010) Positive Steady States of a Diffusive Predator Prey System with Modified Holling Tanner Functional Response. *Nonlinear Analysis*: *Real World Applications*, **11**, 3711-3721.

https://doi.org/10.1016/j.nonrwa.2010.02.001

[10] Li, M.F., Han, B., Xu, L. and Zhang, G. (2013) Spiral Patterns Near Turing Instability in a Discrete Reaction Diffusion System. *Chaos, Solitons & Fractals*, **49**, 1-6. https://doi.org/10.1016/j.chaos.2013.01.010

[11] Mukhopadhyay, B. and Bhattacharyya, R. (2006) Modeling the Role of Diffusion Coefficients on Turing Instability in a Reaction Diffusion Prey Predator System. *Bulletin of Mathematical Biology*, **68**, 293-313. https://doi.org/10.1007/s11538-005-9007-2

[12] Hsu, S.B. and Huang, T.W. (1995) Global Stability for a Class of Predator Prey Systems. *SIAM Journal on Applied Mathematics*, **55**, 763-783. https://doi.org/10.1137/S0036139993253201

[13] Fedoseyev, A.I., Friedman, M.J. and Kansa, E.J. (2002) Improved Multiquadric Method for Elliptic Partial Differential Equations via PDE Collocation on the Boundary. *Computers & Mathematics with Applications*, **43**, 439-455. https://doi.org/10.1016/S0898-1221(01)00297-8

[14] Hioe, F.T. (1999) Solitary Waves for N Coupled Nonlinear Schrodinger Equations. *Physical Review Letters*, **82**, 1152-1155. https://doi.org/10.1103/PhysRevLett.82.1152

[15] Ahmed, B. (2012) 1-Soliton Solution for Zakharov Equations. *Advanced Studies in Theoretical Physics*, **6**, 457-466.

[16] Bao, W. and Yang, L. (2007) Efficient and Accurate Numerical Methods for the Klein-Gordon-Schrödinger Equations. *Journal of Computational Physics*, **225**, 1863-1893. https://doi.org/10.1016/j.jcp.2007.02.018

[17] Hu, G.P., Li, X.L. and Wang, Y.P. (2015) Pattern Formation and Spatiotemporal Chaos in a Reaction—Diffusion Predator—Prey System. *Nonlinear Dynamics*, **81**, 265-275. https://doi.org/10.1007/s11071-015-1988-2

[18] Banerjee, M. and Banerjee, S. (2012) Turing Instabilities and Spatio-Temporal Chaos in Ratio-Dependent Holling-Tanner Model. *Mathematical Biosciences*, **236**, 64-76. https://doi.org/10.1016/j.mbs.2011.12.005

International Journal of Modern Nonlinear Theory and Application, 2023, 12, 68-80
https://www.scirp.org/journal/ijmnta
ISSN Online: 2167-9487
ISSN Print: 2167-9479

Galerkin Method for Numerical Solution of Volterra Integro-Differential Equations with Certain Orthogonal Basis Function

Omotayo Adebayo Taiwo[1], Liman Kibokun Alhassan[1], Olutunde Samuel Odetunde[2], Olatayo Olusegun Alabi[3]

[1]Department of Mathematics, University of Ilorin, Ilorin, Nigeria
[2]Department of Mathematical Sciences, Olabisi Onabanjo University, Ago-Iwoye, Nigeria
[3]Department of Statistics, Federal University of Technology, Akure, Nigeria
Email: tayo@unilorin.edu.ng, limanalhassan@icloud.com, tuned.odetunde@oouagoiwoye.edu.ng, alabioo@futa.edu.ng

How to cite this paper: Taiwo, O.A., Alhassan, L.K., Odetunde, O.S. and Alabi, O.O. (2023) Galerkin Method for Numerical Solution of Volterra Integro-Differential Equations with Certain Orthogonal Basis Function. *International Journal of Modern Nonlinear Theory and Application*, **12**, 68-80.
https://doi.org/10.4236/ijmnta.2023.122005

Received: April 4, 2023
Accepted: June 27, 2023
Published: June 30, 2023

Abstract

This paper concerns the implementation of the orthogonal polynomials using the Galerkin method for solving Volterra integro-differential and Fredholm integro-differential equations. The constructed orthogonal polynomials are used as basis functions in the assumed solution employed. Numerical examples for some selected problems are provided and the results obtained show that the Galerkin method with orthogonal polynomials as basis functions performed creditably well in terms of absolute errors obtained.

Keywords

Galerkin Method, Integro-Differential Equation, Orthogonal Polynomials, Basis Function, Approximate Solution

1. Introduction

Integro-differential equations (IDEs) have attracted growing interest over the years because of the mathematical application in real life problems. Mathematical modeling of real life problems usually resulted in fractional equations. Many mathematical formulations of physical phenomena contain integro-differential equations. These equations arise in many fields like Physics, Astronomy, Potential theory, Fluid dynamics, Biological models and Chemical kinetics. Integro-differential equations contain both integral and differential operators. The derivatives of the unknown functions may appear to any order (see [1] and [2]). [3] obtained solution of an integro-differential equation arising in oscillating magnetic field using Homotopy perturbation method. Galerkin method is a powerful

tool for solving many kinds of equations in various fields of science and engineering. It is one of the most important weighted residual methods inverted by Russians mathematicians Boris Grigoryevrich Galerkin. Recently, various Galerkin algoriyhm have been applied in numerical solution of integral and integro-differential equations. The following methods that are based on the Galerkin ideas, includes Galerkin Finite Element [4], iterative Galerkin with hybrid functions [5], Crank-Nicolson least squares Galerkin [6], and Legendre Galerkin [7]. [8] published a note on three numerical procedures to solve Volterra integro-differential equations on structural analysis.

2. Problem Considered

We consider the higher order linear integro-differential equation as follows:

$$\sum_{i=0}^{n} P_i y^{(i)} + \lambda \int_{g(x)}^{h(x)} k(x,t)\, y(t)\, \mathrm{d}t = f(x) \tag{1}$$

Subject to the following conditions

$$y^{(k)}(a) = \alpha_k, k = 1,2,\cdots,n \tag{2}$$

where $\alpha_k (k \geq 0)$ are constant coefficients, $g(x)$ and $h(x)$ are lower and upper limits of integration, λ is a constant parameter and $k(x,t)$ is a function of two variables *x* and *t* called the kernel, $f(x)$ is a known function and $y(x)$ is the unknown function to be determined.

3. Definitions

Integro-differential equation

An integro-differential equation is an equation involving both integral and derivatives of a function. Example of such equation is stated below:

$$a_2 y''(x) + a_1 y'(x) + a_0 y(x) + \lambda \int_a^b H(x,t)\, y(t)\, \mathrm{d}t = f(x) \tag{3}$$

Galerkin method

Galerkin method is a method of determining coefficient a_k in a power series solution of the form:

$$y(x) \cong y_0(x) + \sum_{k=0}^{n} a_k y_k(x) \tag{4}$$

of the ordinary differential equation $L[y(x)] = 0$ so that $L[y(x)]$, the result of applying the ordinary differential operator to $y(x)$, is orthogonal to every $y_k(x)$ for $k = 1,2,\cdots,n$

Chebyshev Polynomial

The Chebyshev polynomials of the first kind are a set of orthogonal polynomials defined as the solutions to the Chebyshev differential equation and denoted by $T_n(x)$. The Chebyshev polynomial of the first kind denoted by $T_n(x)$ is defined by the contour integral

$$T_n(x) = \frac{1}{4\pi i} \oint \frac{\left(1-t^2\right) t^{-n-1}}{\left(1-2tz+t^2\right)} \mathrm{d}t$$

Where the contour encloses the origin and is traversed in a counter clockwise direction.

Orthogonal over a set

A set of function $\{\phi_r(x)\}$ is said to be orthogonal over a set of points $\{x_i\}$ with respect to the weight function $w(x)$, if

$$\sum_{i=0}^{N} w(x_i)\phi_j(x_i)\phi_k(x_i) = 0,\ i \neq k$$

Orthogonal over an interval

A set of functions $\{\phi_r(x)\}$ is said to orthogonal on an interval $[a,b]$ with respect to the weight function $w(x)$, if

$$\int_a^b w(x)\phi_i(x)\phi_j(x)\mathrm{d}x = 0,\ i \neq j$$

Approximate solution

Approximate solution is used for the expression obtained after the unknown constants have been generated and substituting back into the assumed solution. It is hereby call approximate solution since it is a reasonable approximation to the exact solution.

4. Construction of Orthogonal Polynomials

In this section, we constructed orthogonal polynomials $f_i(x)$, valid on the interval $[a,b]$ with the leading term x^i

Then, starting with

$$f_0(x) = 1, \tag{5}$$

Thus, we find the linear polynomials $f_1(x)$, with leading term *x*, is written as

$$f_1(x) = x + k_{1,0} f_0(x), \tag{6}$$

where, $k_{1,0}$ is a constant to be determined. Since $f_0(x)$ and $f_1(x)$ are orthogonal, we have,

$$\int_a^b w(x) f_0(x) f_1(x)\mathrm{d}x = 0 = \int_a^b x w(x) f_0(x)\mathrm{d}x + k_{1,0}\int_a^b w(x)\left(f_0(x)\right)^2\mathrm{d}x$$

using (5) and (6).

From the above, we have,

$$k_{1,0} = -\frac{\int_a^b x w(x) f_0(x)}{\int_a^b w(x)\left(f_0(x)\right)^2}\mathrm{d}x$$

Hence, (6) gives,

$$f_1(x) = x - \frac{\int_a^b x w(x) f_0(x)}{\int_a^b w(x)\left(f_0(x)\right)^2}\mathrm{d}x$$

Now, the polynomials $f_2(x)$, of degree 2 and the leading term x^2 is written as

$$f_2(x) = x^2 + k_{2,0} f_0(x) + k_{2,1} f_1(x) \tag{7}$$

where the constants $k_{2,0}$ and $k_{2,1}$ are determined by using orthogonality conditions

$$\int_a^b w(x) f_p(x) f_q(x) \mathrm{d}x = \begin{cases} 0, & p \neq q \\ \int_a^b w(x) f_p^2(x) \mathrm{d}x, & p = q \end{cases} \tag{8}$$

Since $f_2(x)$ is orthogonal to $f_0(x)$, we have

$$\int_a^b w(x) f_0(x) \left[x^2 + k_{2,0} f_0(x) + k_{2,1} f_1(x) \right] \mathrm{d}x = 0 \tag{9}$$

Since,

$$\int_a^b w(x) f_0(x) f_1(x) \mathrm{d}x = 0$$

The above equation gives

$$k_{2,0} = -\frac{\int_a^b x^2 w(x) f_0(x)}{\int_a^b w(x) \left(f_0(x) \right)^2} \mathrm{d}x = -\frac{\int_a^b x^2 w(x) \mathrm{d}x}{\int_a^b w(x) \mathrm{d}x} \tag{10}$$

Again, since $f_2(x)$ is orthogonal to $f_1(x)$, we have

$$\int_a^b w(x) f_1(x) \left[x^2 + k_{2,0} f_0(x) + k_{2,1} f_1(x) \right] \mathrm{d}x = 0$$

Thus, using (7), we obtain

$$k_{2,1} = -\frac{\int_a^b x^2 w(x) f_1(x)}{\int_a^b w(x) \left(f_1(x) \right)^2} \mathrm{d}x \tag{11}$$

Since $k_{2,1}$ and $k_{2,0}$ are known, (7) determines $f_2(x)$. Proceeding in the same way, the method is generalized and we have,

$$f_j(x) = x^j + k_{j,0} f_0(x) + k_{j,1} f_1(x) + \cdots + k_{j,j-1} \tag{12}$$

where the constants $k_{j,i}$ and so chosen that $f_j(x)$ is orthogonal to

$$f_0(x), f_1(x), \cdots, f_{j-1}(x)$$

These conditions yield,

$$k_{j,i} = -\frac{\int_a^b x^j w(x) f_i(x)}{\int_a^b w(x) \left(f_i(x) \right)^2} \mathrm{d}x \tag{13}$$

Few terms of orthogonal polynomials valid in the interval [−1, 1] are given below.

$$f_0(x) = 1$$
$$f_1(x) = x$$
$$f_2(x) = x^2 - \frac{1}{3}$$
$$f_3(x) = x^3 - \frac{3}{5}x$$
$$f_4(x) = x^4 - \frac{6}{7}x^2 + \frac{3}{35}$$
$$\vdots$$

etc.

5. Demonstration of Orthogonal Galerkin Method on General Problem Considered

In this section, we considered (1) and (2).

Here we assumed an approximate solution of the form

$$u(x) \cong u_N(x) = \sum_{i=0}^{N} a_i f_i(x), \quad -1 \le x \le 1 \tag{14}$$

where $f_i(x)(i \ge 0)$ are the orthogonal polynomial constructed and valid in the interval [−1, 1].

Thus, differentiating (14)/with respect to *x*, *n* times, we have

$$u^{(n)}(x) \cong u_N^{(n)}(x) = \sum_{i=0}^{N} a_i f_i^{(n)}(x) \tag{15}$$

Substituting (14) and (15) into (1), we obtain

$$\sum_{k=0}^{n}\sum_{i=0}^{N} P_k a_i f_i^{(n)}(x) = f(x) + \lambda \sum_{i=0}^{N} a_i \int_0^x k(x,t) \sum_{i=0}^{N} f_i(t) \mathrm{d}t \tag{16}$$

We determined the unknown coefficients a_i using the Galerkin idea by multiplying both sides of (16) by $f_j(x)$ and then integrating with respect to *x* from −1 to 1.

Thus, we obtain

$$\begin{aligned} &\sum_{k=0}^{n}\sum_{i=0}^{N} P_k a_i \int_{-1}^{1} f_i^{(n)}(x) f_j(x) \mathrm{d}x \\ &= \int_{-1}^{1} f_j(x) f(x) \mathrm{d}x + \lambda \sum_{i=0}^{N} a_i \int_0^x \int_{-1}^{1} k(x,t) \sum_{i=0}^{N} f_i(t) f_j(x) \mathrm{d}t \mathrm{d}x, \quad j = 0,1,\cdots,N \end{aligned} \tag{17}$$

This process generates a system of linear equations for the unknown $\{a_i\}_{i=0}^{N}$ together with the conditions

$$\sum_{i=0}^{N} a_i f_i^{(j)}(a) = \alpha_j, \quad j = 1,2,\cdots,n \tag{18}$$

for the same number of equations in the linear system.

The unknown parameters are determined by solving the system (17) and (18). The values of the constants obtained are then substituted back into (14) to get the required approximate solution for the appropriate order.

6. Numerical Experiments

In this section, we consider four selected problems for experimenting and compare our results with existing results.

Numerical example 1

We consider the Volterra integro-differential equations of the second kind of the form:

$$y'(x) = 1 - 2x\sin x + \int_0^x y(t) \mathrm{d}t \tag{19}$$

together with the condition given as

$$y(0)=0 \tag{20}$$

The exact solution is given as

$$y(x)=x\cos x$$

Here we solved example 1 for case $N=4$.

Thus, Equation (14) becomes

$$y_4(x)=\sum_{i=0}^{4}a_i f_i(x) \tag{21}$$

Substituting the values of $f_i(x), 0\le i\le 4$, we obtain

$$\begin{aligned} y_4(x)=a_0+(2x-1)a_1+\left((2x-1)^2-\frac{1}{3}\right)a_2+\left((2x-1)^3-\frac{3}{5}(2x-1)\right)a_3 \\ +\left((2x-1)^4-\frac{6}{7}(2x-1)^2+\frac{3}{35}\right)a_4 \end{aligned} \tag{22}$$

and,

$$y_4'(x)=2a_1+(8x-4)a_2+\left(6(2x-1)^2-\frac{6}{5}\right)a_3+\left(8(2x-1)^3-\frac{48}{7}x+\frac{24}{35}\right)a_4 \tag{23}$$

Substituting (23) into (19) for case $N=4$, we obtain

$$\begin{aligned} &2a_1+(8x-4)a_2+\left(6(2x-1)^2-\frac{6}{5}\right)a_3+\left(8(2x-1)^3-\frac{48}{7}x+\frac{24}{35}\right)a_4 \\ &-\int_a^x\left\{a_0+(2t-1)a_1+\left((2t-1)^2-\frac{1}{2}\right)a_2+\left((2t-1)^3-\frac{3}{5}(2t-1)\right)a_3\right. \\ &\left.+\left((2t-1)^4-\frac{6}{7}(2t-1)^2+\frac{3}{35}\right)a_4\right\}\mathrm{d}t=1-2x\sin x \end{aligned} \tag{24}$$

Thus, evaluating the integral in (24) and simplifying, we obtain

$$\begin{aligned} &-xa_0+\left(2+x-x^2\right)a_1+\left(\frac{15}{2}x+2x^2-\frac{4}{3}x^3+4\right)a_2 \\ &+\left(6(2x-1)^2+\frac{2}{3}x-2x^4+4x^3-\frac{12}{5}x^2-\frac{6}{5}\right)a_3 \\ &+\left(8(2x-1)^3-\frac{248}{35}x-\frac{16}{5}x^5+8x^4-\frac{48}{7}x^3+\frac{16}{7}x^2+\frac{24}{35}\right)a_4=1-2x\sin x \end{aligned} \tag{25}$$

The unknown coefficients $a_i(i\le 4)$ are determined using the Galerkin idea by multiplying both sides of (25) by $f_j(2x-1)$ and then integrating the resulted equation between $x=-1$ to $x=1$.

For case $j=1$, we multiplied both sides of (25) by $(2x-1)$ and then integrating the resulted equation between $x=-1$ to $x=1$, to obtain

$$-\frac{4}{3}a_0-2a_1-\frac{2}{5}a_2-\frac{460}{9}a_3+\frac{6032}{35}a_4=-0.7953 \tag{26}$$

For case $j=2$, we multiplied both sides of (25) by $(2x-1)^2-\frac{1}{3}$ and then integrating the resulted equation between $x=-1$ to $x=1$, to obtain

$$\frac{8}{3}a_0+\frac{148}{45}a_1+\frac{20}{9}a_2+\frac{183272}{1575}a_3-\frac{128032}{315}a_4=0.363 \tag{27}$$

For case $j=3$, we multiplied both sides of (25) by $(2x-1)^3-\frac{3}{5}(2x-1)$ and then integrating the resulted equation between $x=-1$ to $x=1$, to obtain

$$-\frac{32}{5}a_0-\frac{92}{15}a_1-\frac{1544}{525}a_2-\frac{20776}{75}a_3+\frac{11053408}{11025}a_4=0.18 \tag{28}$$

For case $j=4$, we multiplied both sides of (25) by $(2x-1)^4-\frac{6}{7}(2x-1)^2+\frac{3}{35}$ and then integrating the resulted equation between $x=-1$ to $x=1$, to obtain

$$\frac{1664}{105}a_0+\frac{432}{35}a_1+\frac{416}{105}a_2+\frac{2518688}{3675}a_3-\frac{124288}{49}a_4=-2.3 \tag{29}$$

Now, using the condition given in (22), we obtain

$$a_0-a_1+\frac{2}{3}a_2-\frac{2}{5}a_3+\frac{8}{25}a_4=0 \tag{30}$$

Hence, (26)-(30) are then solved to obtain the unknown constants $a_i\,(i=0,1,2,3,4)$ which are then substituted to the approximate Equation (22).

Again, we solved (1) and (2) for case $N=6$ by re-writing (21) as:

$$y_6(x)=\sum_{i=0}^{6}a_i f_i(x) \tag{31}$$

Hence, (31) becomes

$$\begin{aligned}y_6(x)=a_0+(2x-1)a_1&+\left((2x-1)^2-\frac{1}{3}\right)a_2\\&+\left((2x-1)^3-\frac{3}{5}(2x-1)\right)a_3\\&+\left((2x-1)^4-\frac{6}{7}(2x-1)^2+\frac{3}{35}\right)a_4\\&+\left((2x-1)^5-\frac{10}{9}(2x-1)^3+\frac{5}{21}(2x-1)\right)a_5\\&+\left((2x-1)^6-\frac{15}{11}(2x-1)^4+\frac{5}{11}(2x-1)^2-\frac{5}{231}\right)a_6\end{aligned} \tag{32}$$

And,

$$\begin{aligned}y_6'(x)=2a_1+(8x-4)a_2&+\left(6(2x-1)^2-\frac{6}{5}\right)a_3\\&+\left(8(2x-1)^3-\frac{48}{7}x+\frac{24}{35}\right)a_4\\&+\left(10(2x-1)^4-\frac{20(2x-1)^3}{3}+\frac{10}{21}\right)a_5\\&+\left(12(2x-1)^5-\frac{120(2x-1)^3}{11}+\frac{40x}{11}-\frac{20}{11}\right)a_6\end{aligned} \tag{33}$$

Thus substituting (32) and (33) into (19), we obtain

$$
\begin{aligned}
&2a_1+(8x-4)a_2+\left(6(2x-1)^2-\frac{6}{5}\right)a_3+\left(8(2x-1)^3-\frac{48}{7}x+\frac{24}{35}\right)a_4\\
&+\left(10(2x-1)^4-\frac{20(2x-1)^3}{3}+\frac{10}{21}\right)a_5+\left(12(2x-1)^5-\frac{120(2x-1)^3}{11}+\frac{40x}{11}\right.\\
&\left.-\frac{20}{11}\right)a_6-\int_0^x\left\{a_0+(2t-1)a_1+\left((2t-1)^2-\frac{1}{2}\right)a_2+\left((2t-1)^3-\frac{3}{5}(2t-1)\right)a_3\right.\\
&+\left((2t-1)^4-\frac{6}{7}(2t-1)^2+\frac{3}{35}\right)a_4+\left(10(2t-1)^4-\frac{20(2t-1)^3}{3}+\frac{10}{21}\right)a_5\\
&\left.+\left(12(2t-1)^5-\frac{120(2t-1)^3}{11}+\frac{40t}{11}-\frac{20}{11}\right)a_6\right\}\mathrm{d}t=1-2x\sin x
\end{aligned}
\tag{34}
$$

Thus, evaluating the integral in (34) and simplifying, we obtain

$$
\begin{aligned}
&-xa_0+\left(2+x-x^2\right)a_1+\left(\frac{15}{2}x+2x^2-\frac{4}{3}x^3+4\right)a_2\\
&+\left(6(2x-1)^2+\frac{2}{3}x-2x^4+4x^3-\frac{12}{5}x^2-\frac{6}{5}\right)a_3\\
&+\left(8(2x-1)^3-\frac{248}{35}x-\frac{16}{5}x^5+8x^4-\frac{48}{7}x^3+\frac{16}{7}x^2+\frac{24}{35}\right)a_4\\
&+\left(10(2x-1)^4-\frac{20}{3}(2x-1)^3+\frac{1200}{147}x-32x^5+\frac{280}{3}x^4-\frac{320}{3}x^3+60x^2\right)a_5\\
&+\left(12(2x-1)^5-\frac{120}{11}(2x-1)^3+\frac{72}{11}x-\frac{1280}{11}x^6+192x^5-\frac{2400}{11}x^4\right.\\
&\left.+\frac{1280}{11}x^3-\frac{320}{11}x^2\right)a_6=1-2x\sin x
\end{aligned}
\tag{35}
$$

The unknown coefficients $a_i\left(i\le 4\right)$ are determined using the Galerkin idea by multiplying both sides of (35) by $f_j\left(2x-1\right)$ and then integrating the resulted equation between $x=-1$ to $x=1$.

For case $j=1$, we multiplied both sides of (35) by $(2x-1)$ and then integrating the resulted equation between $x=-1$ to $x=1$, to obtain

$$
-\frac{4}{3}a_0-2a_1-\frac{2}{5}a_2-\frac{460}{9}a_3+\frac{6032}{35}a_4-\frac{97264}{189}a_5+\frac{360160}{231}a_6=-0.7953 \tag{36}
$$

For case $j=2$, we multiplied both sides of (35) by $\left(2x-1\right)^2-\frac{1}{3}$ and then integrating the resulted equation between $x=-1$ to $x=1$, to obtain

$$
\frac{8}{3}a_0+\frac{148}{45}a_1+\frac{20}{9}a_2+\frac{183272}{1575}a_3-\frac{128032}{315}a_4+\frac{238816}{189}a_5-\frac{1507904}{385}a_6=0.363 \tag{37}
$$

For case $j=3$, we multiplied both sides of (35) by $\left(2x-1\right)^3-\frac{3}{5}\left(2x-1\right)$ and then integrating the resulted equation between $x=-1$ to $x=1$, to obtain

$$
\begin{aligned}
&-\frac{32}{5}a_0-\frac{92}{15}a_1-\frac{1544}{525}a_2-\frac{20776}{75}a_3+\frac{11053408}{11025}a_4-\frac{1007648}{315}a_5\\
&+\frac{2330560}{231}a_6=0.18
\end{aligned}
\tag{38}
$$

For case $j=4$, we multiplied both sides of (35) by $(2x-1)^4-\frac{6}{7}(2x-1)^2+\frac{3}{35}$ and then integrating the resulted equation between $x=-1$ to $x=1$, to obtain

$$\frac{1664}{105}a_0+\frac{432}{35}a_1+\frac{416}{105}a_2+\frac{2518688}{3675}a_3-\frac{124288}{49}a_4+\frac{360321152}{47659}a_5 -\frac{63937952}{24255}a_6=-2.3 \tag{39}$$

For case $j=5$, we multiplied both sides of (25) by $(2x-1)^5-\frac{10}{9}(2x-1)^3+\frac{5}{21}(2x-1)$ and then integrating the resulted equation between $x=-1$ to $x=1$, to obtain

$$-\frac{2528}{63}a_0-\frac{4976}{180}a_1+\frac{2720}{7}a_2-\frac{550112}{315}a_3+\frac{1396705664}{218295}a_4-\frac{85672064}{3969}a_5 +\frac{48377661184}{693693}a_6=-\frac{3152}{63}-\frac{2002592}{63}\cos(1)+\frac{144}{7} \tag{40}$$

For case $j=6$, we multiplied both sides of (35) by $(2x-1)^6-\frac{15}{11}(2x-1)^4+\frac{5}{11}(2x-1)^2-\frac{5}{231}$ and then integrating the resulted equation between $x=-1$ to $x=1$, to obtain

$$-\frac{2528}{63}a_0-\frac{4976}{180}a_1+\frac{2720}{7}a_2-\frac{550112}{315}a_3+\frac{1396705664}{218295}a_4-\frac{85672064}{3969}a_5 +\frac{48377661184}{693693}a_6=-\frac{1376}{11}-\frac{230568512}{231}\cos(1)+\frac{1290272}{63}\sin(1) \tag{41}$$

Now, using the condition given in (22), we obtain

$$a_0-a_1+\frac{2}{3}a_2-\frac{2}{5}a_3+\frac{8}{25}a_4-\frac{8}{63}a_5+\frac{16}{231}a_6=0 \tag{42}$$

Hence, (36)-(42) are then solved to obtain the unknown constants $a_i\,(i=0,1,2,3,4,5,5,6)$ which are then substituted to the approximate equation (32). More values of N are computed follow the same procedure and the results obtained are tabulated below.

Example 2:

$$y''(x)+xy'(x)-xy(x)=\mathrm{e}^x-2\sin x+\int_{-1}^{1}y(t)\mathrm{d}t$$

With the conditions

$y(0)=1$ and $y'(0)=1$, The exact solution is $y(x)=\mathrm{e}^x$.

Example 3: Consider the Fredholm integro-differential equation (See [2])

$$y''''(x)=1+\int_0^1\mathrm{e}^{-x}y^2(t)\mathrm{d}t,\quad 0<x<1$$

Together with the conditions $y(0)=y'(0)=1$; $y(1)=\mathrm{e}$; $y'(1)=\mathrm{e}$. The exact solution is $y(x)=\mathrm{e}^x$.

- **Denotes the results are not available for comparison**
- **Denotes Results are not available for comparison**

Example 4: Consider the Fredholm integro-differential equation (See [2])

$$y''''(x)=x+(x+3)\mathrm{e}^x+y(x)-\int_0^x y(t)\mathrm{d}t,\quad 0<x<1$$

With the following conditions
$y(0)=1$; $y(1)=1+\mathrm{e}$; $y''(0)=2$; $y''(1)=3\mathrm{e}$. The exact solution is $y(x)=1+x\mathrm{e}^{x}$.

- **Denotes Results are not available for comparison**
- **Denotes Results are not available for comparison**

7. Discussion of Results

The approximate solution obtained by means of Galerkin method is a finite power series which can be in turn expressed in closed form of exact solution as the degree of the approximant increases. The finite series solution is obtained for each problem considered by increasing the value of *N*, which in turn converges to closed form of exact solution, the absolute errors obtained tend to zero and ensures stability of our method (See Tables 1-8). Also, from the results obtained by [2], our method proved superior to [2]. As *N* increases, the results obtained in some cases converged. It proves a very efficient method for the problems attempted, for which the form of the solution is known.

Table 1. Numerical results and absolute errors of example 1 for case $N=4$.

X	Exact solution	Approximate solution	Approximate solution
0	0	0	0
0.1	0.09999984769	0.1007787777	7.7893×10^{-4}
0.2	0.19999871500	0.20007989915	8.0021×10^{-4}
0.3	0.29999588772	0.30082048742	8.2460×10^{-4}
0.4	0.39990252364	0.40085698231	9.5446×10^{-4}
0.5	0.49998096153	0.50093900554	9.5813×10^{-4}
0.6	0.59996710167	0.60128870164	1.2920×10^{-3}
0.7	0.69994775882	0.70214095881	2.1932×10^{-3}
0.8	0.79992201922	0.80415158192	4.2296×10^{-3}
0.9	0.89988896922	0.90630266921	6.4113×10^{-3}
1.0	0.99984769523	1.00008011995	2.3242×10^{-4}

Table 2. Numerical results and absolute errors of example 1 for case $N=6$.

X	Exact solution	Approximate solution	Approximate solution
0	0	0	0
0.1	0.09999984769	0.1000123167	1.2409×10^{-5}
0.2	0.19999871500	0.2000261375	2.7350×10^{-5}
0.3	0.29999588772	0.3000306197	3.4732×10^{-5}
0.4	0.39990252364	0.4000469833	5.6731×10^{-5}
0.5	0.49998096153	0.5000608685	7.9907×10^{-5}
0.6	0.59996710167	0.6000487216	8.1620×10^{-5}
0.7	0.69994775882	0.7000377598	9.0001×10^{-5}
0.8	0.79992201922	0.8003215592	3.9951×10^{-5}
0.9	0.89988896922	0.9002501792	3.6121×10^{-5}
1.0	0.99984769523	1.0003425534	5.5778×10^{-5}

Table 3. Numerical results and absolute errors of example 2 for case $N = 4$.

X	Exact solution	Approximate solution	Approximate solution
−1	0.36787944	0.37418684	6.3074×10^{-3}
−0.8	0.44932896	0.45641056	7.0816×10^{-3}
−0.6	0.54881164	0.55712374	8.3121×10^{-3}
−0.4	0.67032005	0.68009815	9.7781×10^{-3}
−0.2	0.81873075	0.82014445	1.4137×10^{-2}
0	1.00000000	1.00180376	1.8937×10^{-2}
0.2	1.22140283	1.24357182	2.2169×10^{-3}
0.4	1.47182472	1.49774274	2.5918×10^{-2}
0.6	1.82211881	1.85630581	3.4187×10^{-2}
0.8	2.22551000	2.26616893	4.0928×10^{-2}
1.0	2.71828182	2.78212785	6.3846×10^{-3}

Table 4. Numerical results and absolute errors of example 2 for case $N = 4$.

X	Exact solution	Approximate solution	Approximate solution
−1	0.36787944	0.367966169	8.6729×10^{-5}
−0.8	0.44932896	0.449409094	8.0134×10^{-5}
−0.6	0.54881164	0.548889417	7.7837×10^{-5}
−0.4	0.67032005	0.676389371	6.9321×10^{-5}
−0.2	0.81873075	0.818758949	7.8199×10^{-5}
0	1.00000000	1.000966532	7.6653×10^{-4}
0.2	1.22140283	1.222229894	8.9614×10^{-4}
0.4	1.47182472	1.472514031	6.8933×10^{-4}
0.6	1.82211881	1.822781972	5.9397×10^{-4}
0.8	2.22551000	2.226029824	4.8892×10^{-4}
1.0	2.71828182	2.718738011	4.5621×10^{-4}

Table 5. Numerical results and absolute errors of example 3 for case $N = 4$.

X	Exact	Approximate of [2]	Approx. of Our Method	Absolute errors of [2]	Absolute errors of Our Method
0.0	1.0000000	1.0000000	1.00000000	0	0
0.1	1.105171		1.105173451	*	2.451×10^{-6}
0.2	1.2214027	1.2214	1.221409351	1.0270×10^{-4}	6.651×10^{-6}
0.3	1.349859	*	1.349868872	*	9.872×10^{-6}
0.4	1.4918246	1.4918	1.491856800	1.1246×10^{-3}	3.220×10^{-5}
0.5	1.648721	*	1.648800850	*	7.985×10^{-5}
0.6	1.8221188	1.8221	1.822700800	6.1188×10^{-3}	5.820×10^{-4}
0.7	2.013753	*	2.014370200	*	6.172×10^{-4}
0.8	2.2255409	2.2255	2.228210900	2.0241×10^{-2}	2.670×10^{-3}
0.9	2.459603	*	2.465275000	*	5.672×10^{-3}
1.0	2.71828183	2.7183	2.725281830	5.1282×10^{-2}	7.000×10^{-3}

*Denotes the results are not available for comparison.

Table 6. Numerical results and absolute errors of example 3 for case $N = 10$.

X	Exact	Approximate of [2]	Approx. of Our Method	Absolute errors of [2]	Absolute errors of Our Method
0.0	1.0000000	1.0000	1.00000000000	0	0
0.1	1.105171	*	1.10517109874	*	9.874×10^{-8}
0.2	1.2214027	1.2214	1.22140278125	2.700×10^{-6}	8.125×10^{-8}
0.3	1.349859	*	1.34985906846	*	6.845×10^{-8}
0.4	1.4918246	1.4918	1.49182466533	2.460×10^{-5}	5.329×10^{-8}
0.5	1.648721	*	1.64872104101	*	4.101×10^{-8}
0.6	1.8221188	1.8221	1.82211884674	1.880×10^{-5}	4.674×10^{-8}
0.7	2.013753	*	2.01375304115	*	4.115×10^{-8}
0.8	2.2255409	2.2255	2.22554093985	4.090×10^{-5}	3.985×10^{-8}
0.9	2.459603	*	2.45960302679	*	2.679×10^{-8}
1.0	2.71828183	2.7183	2.71828184068	1.820×10^{-5}	1.068×10^{-8}

*Denotes the results are not available for comparison.

Table 7. Numerical results and absolute errors of example 4 for case $N = 4$.

X	Exact	Approx. of [2]	Approx. of Our Method	Absolute errors of [2]	Absolute errors of Our Method
0.0	1.0000000	1.0000	1.0000000000	0	0
0.1	1.110517	*	1.1105179874	*	9.874×10^{-7}
0.2	1.2442805	1.244	1.2442922210	2.8055×10^{-4}	1.172×10^{-6}
0.3	1.404958	*	1.4049590990	*	1.099×10^{-6}
0.4	1.5967298	1.592	1.4967570200	2.7299×10^{-4}	9.722×10^{-5}
0.5	1.824361	*	1.8244327200	*	7.172×10^{-5}
0.6	2.0932712	2.068	2.0933164710	2.5270×10^{-2}	4.527×10^{-5}
0.7	2.409627	*	2.4096387200	*	1.172×10^{-5}
0.8	2.7804327	2.696	2.7805028800	8.4430×10^{-2}	9.018×10^{-4}
0.9	3.213943	*	3.2140147700	*	7.177×10^{-4}
1.0	3.71828183	3.5	2.7183814900	2.1820×10^{-1}	6.966×10^{-4}

*Denotes the results are not available for comparison.

Table 8. Numerical results and absolute errors of example 4 for case $N = 10$.

X	Exact	Approx. of [2]	Approx. of Our Method	Absolute errors of [2]	Absolute errors of Our Method
0.0	1.0000000	1.0000	1.000000000000	0	0
0.1	1.110517	*	1.1105170009231	*	9.231×10^{-10}
0.2	1.2442805	1.2443	1.2442805007638	1.950×10^{-5}	7.638×10^{-10}
0.3	1.404958	*	1.4049580006618	*	6.618×10^{-10}
0.4	1.5967298	1.5967	1.5967298002963	3.000×10^{-10}	2.963×10^{-10}
0.5	1.824361	*	1.8243610001316	*	1.316×10^{-10}
0.6	2.0932712	2.0933	2.0932712009316	1.772×10^{-8}	9.316×10^{-9}
0.7	2.409627	*	2.4096270492700	*	4.927×10^{-8}
0.8	2.7804327	2.7804	2.7804327297800	3.214×10^{-7}	2.978×10^{-8}
0.9	3.213643	*	3.2136430198200	*	1.982×10^{-8}
1.0	3.71828183	3.7184	2.7182827690000	1.820×10^{-5}	9.390×10^{-7}

*Denotes the results are not available for comparison.

8. Conclusion

In this work, we have proposed the Galerkin method for solving both the boundary and initial value problems for a class of higher order linear and nonlinear Volterra and Fredholm integro-differential based on the constructed orthogonal polynomials as basis function. Illustrative examples are included to demonstrate the validity and applicability of the technique and the tables of results presented reveal that the absolute error decreases when the degree of approximation increases. Furthermore, since basis functions constructed are polynomials, the values of the integrals for the nonlinear integro differential equations are calculated as approximately close to the exact solutions.

Conflicts of Interest

The authors declare no conflicts of interest regarding the publication of this paper.

References

[1] Atkinson, K. (1997) Numerical Solution of Integral Equation of the Second Kind. Cambridge University Press, Cambridge. https://doi.org/10.1017/CBO9780511626340

[2] Venkatesh, S.G., Ayyaswamy, S.K. and Raja Balachandar, S. (2012) Legendre Approximation Solution for a Class of Higher-Order Volterra Integro-Differntial Equations. *Ain Shams Engineering Journal*, **3**, 417-422. https://doi.org/10.1016/j.asej.2012.04.007

[3] Dehghan, M. and Shakeri, F. (2008) Solution of an Integro-Differential Arising in Oscillating Magnetic Field Using Homotopy Perturbation Method. *Progressive in Electromagnetic Research*, **78**, 361-376. https://doi.org/10.2528/PIER07090403

[4] Jangveladze, T., Kiguradz, Z. and Neto, B. (2011) Galerkin Finite Element Method for One Non-Linear Integro-Differential Model. *Applied Mathematics and Computation*, **217**, 6883-6892. https://doi.org/10.1016/j.amc.2011.01.053

[5] Maleknejad, K. and Tavassoli-Kajani, M. (2011) Solving Linear Integro-Differential Equations System by Galerkin Method with Hybrid Functions. *Applied Mathematics and Computation*, **150**, 603-612. https://doi.org/10.1016/j.amc.2003.10.046

[6] Ghasemi, T., Tavassol-Kajani, M. and Babolian, E. (2007) Numerical Solution of Nonlinear Integro-Differential Equations. Wave-Galerkin Method and Homotopy Perturbation Method. *Applied Mathematics and Computation*, **188**, 450-455. https://doi.org/10.1016/j.amc.2006.10.001

[7] Fakhar-Izadi, F. and Dehghan, M. (2011) An Efficient Pseudo-Spectral Legendre Galarkin Method for Solving a Nonlinear Integro-Differetial Equations Arising in Population Dynamics. *Mathematical Method for Applied Sciences*, **30**, 1485-1511. https://doi.org/10.1002/mma.2698

[8] Tomassiello, S.A. (2011) A Note on Three Numerical Procedures to Solve Volterra Integro-Differential Equations on Structural Analysis. *Applied Mathematics and Computation*, **62**, 3188-3193. https://doi.org/10.1016/j.camwa.2011.08.031

Call for Papers

International Journal of Modern Nonlinear Theory and Application

ISSN: 2167-9479 (Print) **ISSN: 2167-9487 (Online)**
https://www.scirp.org/journal/ijmnta

International Journal of Modern Nonlinear Theory and Application (***IJMNTA***) is an international peer-reviewed journal dedicated to publishing original papers on all topics related to nonlinear dynamics and its applications such as, electrical, mechanical, civil, and chemical systems and so on. The contributions concerned will be discussion of a practical problem, the formulating nonlinear model, and determination of closed form exact or numerical solutions.

Editor-in-Chief

Prof. Ahmad M. Harb German Jordanian University, Jordan

Editorial Board

Subject Coverage

This journal invites original papers and review papers that address the following issues in modern nonlinear theory and its applications. The interested topics that may be covered, but not limited to:

- Application of Modern Nonlinear Theory in:
  - Biology
  - Business
  - Chemical Systems
  - Electrical and Power Systems
  - Fluid Mechanics
  - Mechanical Systems
  - Medicine
  - Physics
- Applied Mechanics
- Bifurcation and Chaos
- Chaos Control
- Classic Control Systems
- Electrical Drives and Power Electronics
- Fractal Order Systems
- High Dimensional Chaos and Applications
- Intelligent Control Systems (Fuzzy, Neural, Genetic…)
- Nonlinear Control
- Nonlinear Differential Equations and Applications
- Nonlinear Dynamic Stability
- Nonlinear Dynamics
- Nonlinear Mathematical Physics
- Nonlinear Optical Physics & Materials
- Nonlinear Oscillations
- Nonlinear Phenomena
- Nonlinear Science and Numerical Simulation
- Power Systems and Energy
- Security in Communication Systems

We are also interested in: 1) Short Reports—2-5 page papers where an author can either present an idea with theoretical background but has not yet completed the research needed for a complete paper or preliminary data; 2) Book Reviews—Comments and critiques.

Notes for Intending Authors

Submitted papers should not have been previously published nor be currently under consideration for publication elsewhere. Paper submission will be handled electronically through the website. All papers are refereed through a peer review process. For more details about the submission, please access the website.

Website and E-Mail

https://www.scirp.org/journal/ijmnta **E-mail: ijmnta@scirp.org**

What is SCIRP?

Scientific Research Publishing (SCIRP) is one of the largest Open Access journal publishers. It is currently publishing more than 200 open access, online, peer-reviewed journals covering a wide range of academic disciplines. SCIRP serves the worldwide academic communities and contributes to the progress and application of science with its publication.

What is Open Access?

All original research papers published by SCIRP are made freely and permanently accessible online immediately upon publication. To be able to provide open access journals, SCIRP defrays operation costs from authors and subscription charges only for its printed version. Open access publishing allows an immediate, worldwide, barrier-free, open access to the full text of research papers, which is in the best interests of the scientific community.

- High visibility for maximum global exposure with open access publishing model
- Rigorous peer review of research papers
- Prompt faster publication with less cost
- Guaranteed targeted, multidisciplinary audience

Scientific Research Publishing

Website: https://www.scirp.org

Subscription: sub@scirp.org

Advertisement: service@scirp.org